Safety Science 158 (2023) 105992

Contents lists available at ScienceDirect

Safety Science

journal homepage: www.elsevier.com/locate/safety

Takeoff runway overrun risk assessment in aviation safety based on human pilot behavioral characteristics from real flight data

Chongfeng Li [a,b], Ruishan Sun [a], Xing Pan [b,*]

[a] College of Safety Science and Engineering, Civil Aviation University of China, 2898 Jinbei Road, Tianjin 300300, China
[b] School of Reliability and Systems Engineering, Beihang University, 37 Xueyuan Road, Haidian, Beijing 100191, China

ARTICLE INFO

Keywords:
Flight safety
Pilot behavior
Flight data
Time series clustering
Similarity theory
Risk assessment

ABSTRACT

Aviation safety is an important part of safety science and pilot behavior is a major factor in flight safety analysis. However, when analyzing unsafe events, such as runway overrun, majority of studies do not quantify the impact of pilot behavior on flight safety. The aim of this paper is to discover the pilot behavioral characteristics from actual flight data and apply them to construct a takeoff runway overrun risk assessment model. Concretely, the time series clustering is used to mine the pilot behavioral characteristics based on pilot operating data. Then, the similarity theory is introduced to construct a data-based man–machine-environment system expression including pilot behavioral characteristics to get the takeoff distance for the runway overrun risk assessment. The results of case study showed that 3 types of pilot behavioral characteristics were found in selected fleet, which mainly differ in the pilot reaction time after V_R and operation input speed of the control column, and RO is more likely to happen under the combined influence of longer reaction time and slower operation input speed. The proposed method makes full use of real flight data from airlines under different conditions incorporating pilot behavior characteristics and can inform risk analysis of other unsafe events such as hard landing, tail strike, etc.

Abbreviations

A	Aircraft performance parameters [\]
ALT	The altitude of an aircraft relative to the ground [m]
B	Pilot behavior parameters [\]
B	Boundary conditions [\]
CAAC	Civil Aviation Administration of China [\]
CCP	Control column position [deg]
CCP_TS	Time series of control column position [\]
C_D	Drag coefficient [\]
C_L	Lift coefficient [\]
D	Reference datasets
E	Environment parameters [\]
Flap	Flaps configuration [\]
F(X)	Takeoff system expression, $\boldsymbol{F(X)}= \{f_1, f_2,\ldots, f_i\}$ [\]
g	Gravity acceleration [m/s^2]
G	Geometric conditions [\]
IATA	International Air Transport Association [\]
I	Initial conditions [\]
k	*k*-SC clustering number [\]
K	Dimensional conversion factor [\]
m	Gross weight of aircraft [kg]
M	Media conditions [\]
N	The compressor speed ratio of aircraft engine [\]
O	Pilot behavioral characteristics [\]
P	Thrust [N]
P_S	Static pressure [Pa]
QAR	Quick Access Recorder [\]
RO	Runway overrun [\]
S	Takeoff distance [m]
S_W	Wing reference area [m^2]
SOP	Standard Operating Procedure [\]
T_S	Static temperature [°C]
t	Time of operations [s]
V_T	The speed of aircraft relative to the air [m/s]
V_R	The V_T when aircraft starts rotation [m/s]
V_{LOF}	The V_T when aircraft lift-off [m/s]
V_2	The V_T when aircraft's *ALT* over 10.70 m [m/s]
V_G	The speed of aircraft relative to the ground [m/s]
V_W	Tailwind speed [m/s]
ρ	Atmospheric density [Kg/m^3]
μ	Runway friction coefficient [\]

* Corresponding author.
E-mail address: panxing@buaa.edu.cn (X. Pan).

https://doi.org/10.1016/j.ssci.2022.105992
Received 28 July 2022; Received in revised form 3 October 2022; Accepted 25 October 2022
Available online 14 November 2022

φ	Runway inclination (gradient) [deg]
$\boldsymbol{X}$	Dimensionless index of $\boldsymbol{F}(\boldsymbol{X})$, $\boldsymbol{X}=\{x_1, x_2,\ldots, x_i\}$ [\]

1. Introduction

Air transport has contributed to the growth of the social, political, and economic globalization process during the last decade by being one of the fastest and safest methods of long-distance travel. The commercial aviation sector deployed 37 million planes every year and carried 4 billion passengers annually before the current coronavirus pandemic hit, and the number could reach 2019 levels as early as 2024 (Madeira et al., 2021). The fast development has brought safety concerns into aircraft industry, and the increase in workload is not accompanied by a proportional gain in personnel. Therefore, employees are often subjected to an enormous quantity of rigorous requests, under pressured time frames, and complex environments. Moreover, compounded factors, such as career uncertainty and frequent demand for overtime, have contributed to an increasing risk of personnel capabilities detriment and, hence, mistakes in safety sensitive tasks (Santos and Melicio, 2019). These circumstances have been further aggravated by the effects of the current pandemic, where companies had to forgo large portions of their employees in order to reduce cash burns and regain profit margins, while maintaining contractual obligations and preparing for a resurgence of traffic demand. In the current context, therefore, the aviation industry needs to pay more attention to the balance between profit and safety by taking the beforementioned factors into account, especially the human factors. Human factors play a critical role in flight safety system (Dolores, 2018; Reason, 1990). Some researchers have suggested that human pilot error has led to over 60 % of flight accidents (Jarvis and Harris, 2010; Shappell et al., 2017). The statistics of the International Air Transport Association (IATA) from 2016 to 2020 indicated that flight crew factors caused about 46 % of aircraft accidents (IATA, 2021). In China, no fatal accidents happened between 2011 and 2020 while 67.90 % of incidents were derived from the flight crew (CAAC, 2021).

1.1. Human factors and pilot behavioral characteristics

A view expressed widely in the safety literature is that human factors have not always had such a primary place in accident causation but emerged as a residual problem as aircraft became more reliable (Hobbs, 2004). Human factors have always taken the lead as the main latent cause of accidents, and between 70 % and 80 % of all aviation accidents have a human factor somewhere in the chain of causation, according to human factors specialists and aviation researchers (De Sant and De Hilal, 2021). Studies have found pressure, fatigue, miscommunication, and a lack of technical knowledge on crucial personnel such as human pilots, maintenance workers, and air traffic controllers to be some of the main probable causes for aviation mishaps (Jensen, 2017; Lee and Kim, 2018; Lee and Kim, 2018; Thorpe et al., 2022; Volz et al., 2016; Yazgan and Kavsaoğlu, 2017). Therefore, human factors should be examined in order to minimize aviation mishaps, and one access is to understand the pilot behavior (Dekker, 2001; Xu et al., 2022). Pilot Behavior involves factors which affect personal performance but also affect interaction with others, which often defines overall safety performance. Since several specific pilot behaviors have been considered significant contributing factors to many accidents, it is critical to identify the elements that may enhance these pilot performance regarding safety behavior (Chen and Chen, 2014).

The concept of pilot behavioral characteristics ($\boldsymbol{O}$), which reflects the representative maneuvers embedded in their operational inputs to the aircraft that have an impact on the aircraft takeoff system, firstly appeared in the literature (Wang et al., 2013). $\boldsymbol{O}$ is primarily influenced by flight training and pilot behavioral style (Sagberg et al., 2015), so there are differences in $\boldsymbol{O}$ between different airlines even different fleets. From a system safety point of view, the operational risks associated with $\boldsymbol{O}$ are expected to be acceptable, but there are undeniably that $\boldsymbol{O}$ in practice might pose risks to flight operations and cause incidences even accidents (Hong et al., 2011; Wang et al., 2018; Zhu and Tong, 2021). For instance, reference (Wang et al., 2018) has shown that $\boldsymbol{O}$ can have an influence on aircraft long landing as well as hard landing. Therefore, with the gradual increase in equipment reliability, it is important to pay more attention to the influence of $\boldsymbol{O}$ for continuously improving flight safety.

Theoretically, the thorough pilot behavior model can be developed by a detailed human-pilot model included the control-theoretic model, neuromuscular system, and sensory system (Lone and Cooke, 2014; Xu et al., 2017). Nevertheless, it is quite time-consuming and costly for normal airlines to do that. Noteworthily, all commercial airplanes in China are required to install Quick Access Recorders (QAR) or similar flight data recording equipment under the Flight Operations Quality Assurance (FOQA) program of the Civil Aviation Administration of China (CAAC). QAR can record pilot operating data like control column position, throttle resolver angle, flap handle position, and so on, which means it is feasible for us to discover $\boldsymbol{O}$ based on QAR (Sun and Xiao, 2012). Further, by combining aircraft performance data and environmental data of QAR, a human–machine-environment based approach to system safety analysis can be developed to quantify the impact of $\boldsymbol{O}$ on flight safety.

1.2. Runway overrun risk assessment

Runway overrun (RO) is a type of runway excursions considered by the European Aviation Safety Agency (EASA, 2016a, b), which occurs when an aircraft departs the end of the runway surface during a takeoff or a landing and is the most severe among runway excursions (Gandhewar and Sonkusare, 2014). Reference (Bateman, 2008) described that the growth of surrounding buildings, the advent of the turbojet aircraft, and the large increase in air traffic were not totally anticipated before, with all of these contributing to an escalation in overrun and their impact. Due to these reasons, regulatory authorities and the aviation industry continue to investigate ways to improve runway safety (IATA, 2011a, b; ICAO, 2013). It would take more sophisticated tools and methods to achieve breakthrough improvements in commercial aviation, however, since commercial aviation operates at such a high level of safety (Ayres, 2011). Currently, research focuses on assessing RO risk from accident statistics and aircraft performance analysis.

Based on RO statistics, research in the literature has examined variables associated with RO and their categories of severity (Natalia and Salvatore, 2020), probability (Galagedera et al., 2019; Szabo et al., 2017) and operational risk (Galagedera et al., 2020). Specifically, a variety of approaches have been suggested to analyze risks in RO, such as Bayesian-network based (Calle-Alonso et al., 2019), multiple Logistic regression method (Wei et al., 2018), and the frequency model (Moretti et al., 2017b, c; Moretti et al., 2018; Yousefi et al., 2020) which has been applied to quantitative risk assessment of RO in some international airports (Di Mascio et al., 2020; Moretti et al., 2017a). Some studies have already shown that the most frequent causes for RO are inappropriate pilot performance and aircraft condition. For example, the literature (Chang et al., 2016) delivered an empirical study based on experts' evaluation suggests that the most important dimension is the pilot's core ability. Similarly, the report of Netherlands Aerospace Centre shows that the "Crew performance inaccurate" and the "Inaccurate information to crew" show a relatively high frequency of RO occurrence (NLR, 2015). The literature (Moretti et al., 2017b; Moretti et al., 2018) based on statistical analysis concludes that pilot performance is a significant cause of RO, mainly in terms of misunderstanding, inattention, inexperience and wrong maneuver. The Skybrary knowledgebase points to the inappropriate aircraft handling technique as a cause of RO (Skybrary, 2022). While the current study has found that pilot behavior does have an impact on RO risk based on accident statistics, there has been no further analysis of specific pilot behavior characteristics and quantification of their impact on RO risk.

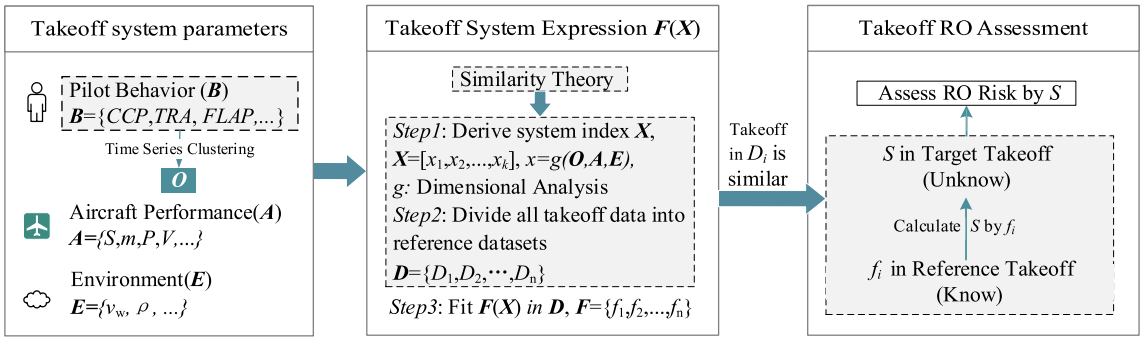

Fig. 1. Overview of the study.

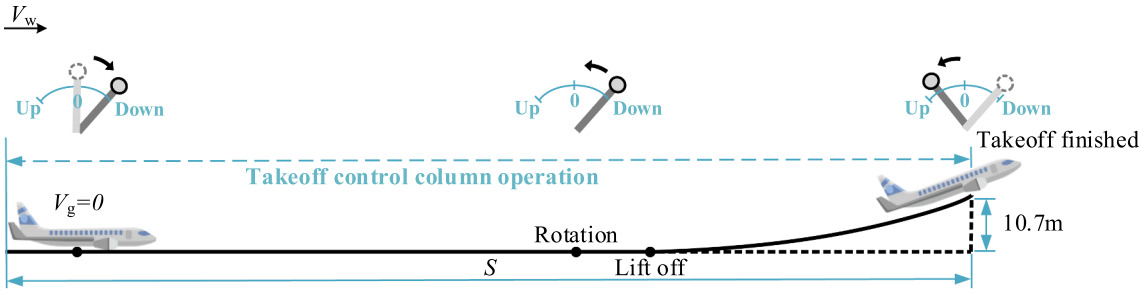

Fig. 2. Takeoff with all engines operating.

Calculation or prediction of operating distances based on aircraft performance analysis is another common access of assessing RO risk. An accurate expression of the dynamics of takeoff system is an important basis for calculating operating distances. In previous studies, aircraft performance analysis based on Newton's Laws of Motion is an important approach to analyze aircraft operation, in which the aircraft takeoff /landing distance is an important parameter as the result of performance analysis to evaluate the risk of RO (Cai et al., 2013; Chen and Xiang, 2013; Song et al., 2007). Meanwhile, considering the uncertainties in actual aircraft operations and the use of vast amounts of flight data, some researches evaluate the aircraft takeoff/landing distance based on artificial intelligence, such as neural network and support vector machine regression (Qian et al., 2017; Ruiying et al., 2017). However, nearly all the above studies regarded human pilot as "standard pilots", which means they assumed that the pilots are all perfect followers of the standard operating procedure (SOP) while ignoring the ***O*** of them. Besides, the artificial intelligence models may have higher accuracy while lacking interpretation and generalization to some extent. In general, airlines require a risk analysis model that clearly reflects the physical mechanism of the unsafety event and can also be widely used by leveraging existing real flight data.

1.3. Aim and structure of study

The objective of this study is to examine the effects of ***O*** on the risk of RO based on real flight data. As shown in Fig. 1, we will mine ***O*** based on the real pilot operational parameters in QAR and calculate the key parameter S of takeoff RO risk evaluation by describing the man–machine-environment system of the takeoff process. The study will help airlines to pay more attention to the potential risk of RO from pilot behavior and to be able to make full use of actual flight data to make a more accurate assessment to reduce the likelihood of high-risk ***O*** causing RO. Our research is divided into the following specific sections. Section 2 implements the construction of the method, including the selection of the QAR parameters, the analysis method of ***O*** and the parameters calculation method of RO risk assessment. Section 3 presents the case study followed by the discussions in Section 4 and the conclusions in Section 5.

2. Method

This section presents the methodological approach to studying the impact of ***O*** on RO. According to Fig. 1, Section 2.2 gives the analysis of ***O*** based on time series clustering algorithm of pilot operating data, and the result ***O*** is used as a parameter in the construction of ***F***(***X***) based on similarity theory in section 2.3. Then, the method are applied to RO risk evaluation by calculating S of ***F***(***X***) in section 2.4. Prior to above analysis, in section 2.1, the main system parameters ***B***, ***A***, ***E*** used in this study are selected based on aircraft takeoff dynamics analysis and pilot operating behavior analysis.

2.1. Model parameters selection

QAR is currently capable of recording hundreds or even thousands of flight parameters, each of which will affect the aircraft operation. Therefore, flight parameters should be selected to highlight the main features of RO in order to improve model interpretation and reduce the cost of the study. In current study, the flight data of takeoff is selected to analyze ***O*** and describe the aircraft takeoff system ***F***(***X***), and the risk of RO is assessed by calculating S in ***F***(***X***). Based on the Newton's Laws of Motion, the aircraft takeoff with all engines is shown in Fig. 2 and the calculation method of S is shown in formula (1).

$$S = \int_{V_W}^{V_R} \frac{m(V - V_W)\mathrm{d}V}{[P - (\mu + \varphi)mg - \frac{1}{2}(C_D - \mu C_L)\rho V^2 S_W]} + K\left(\frac{V_R + V_{LOF}}{2} - V_W\right)(t_{V_R \sim V_2} - t_{V_{LOF} \sim V_2}) + K\left(\frac{V_{LOF} + V_2}{2} - V_W\right)t_{V_{LOF} \sim V_2} \quad (1)$$

It is based on formula (1) that existing studies have investigated S of aircraft by analyzing runway conditions, engine thrust, wind speed and other perspectives under the assumption of standard operating

Table 1
Selection of parameters.

Classification	Symbol	Description
Pilot Behavior(***B***)	*CCP*	The angle of control column deviated from original point
Aircraft Performance(***A***)	m	Gross weight of aircraft
	V_G	The speed of aircraft relative to the ground
	ALT	The altitude of an aircraft relative to the ground
	V_A	The speed of aircraft indicated by instrument
	V_T	The speed of aircraft relative to the air
	V_R	The V_T when aircraft starts rotation
	V_{LOF}	The V_T when aircraft lift-off
	V_2	The V_T when aircraft's *ALT* over 10.70 *m*
	N	The compressor speed ratio of aircraft engine
	P	The thrust of aircraft, which is calculated based on N
	S	The horizontal distance from the point where $V_G = 0$ to $ALT = 10.7$ m, which is the integral of V_G against time
	S_W	Wing reference area
	FLAP	The setting position of flap handle
Environment(***E***)	V_W	The wind speed along the longitudinal axis of the aircraft
	P_S	The static pressure of air
	T_S	The static temperature of air
	ρ	The density of air, calculated by $\rho = \frac{P_S}{RT_S}$, where R = 287.15 J/(kg·k)

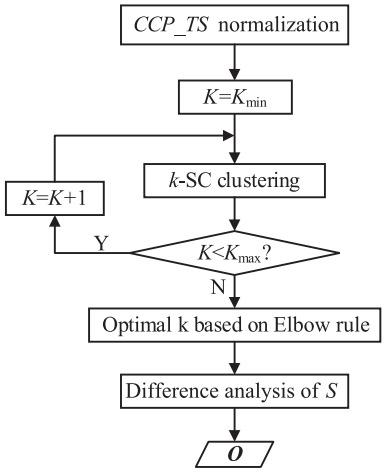

Fig. 3. Pilot behavioral characteristics mining.

procedures (SOP). However, as discussed in introduction, SOP ignores the effect of ***O*** on *S*. For instance, by maneuvering devices like control column and thrust lever, ***O*** can affect V_R, V_{LOF} and V_2, and the variation in engine thrust, C_D and C_L, operation interval, altitude per unit time, etc. If it's not able to identify well the ***O*** that makes *S* increase, the risk RO could rise. Therefore, an analysis of the pilot takeoff maneuvers is required.

As shown in Fig. 2, during takeoff, the pilot accelerates the aircraft by setting required thrust and keeps the control column in Down position which allows the aircraft to accelerate steadily on the runway. At the Rotation point, pilot pulls the control column to make the lift of aircraft greater than gravity and bring the aircraft safely off the ground at the Lift off, the whole takeoff process ends when the aircraft above 10.7 m. It is concluded that the pilot operation of control column dominates the takeoff. Besides, the pilot pushes the thrust lever within almost same speed in current QAR sampling frequency in China, so the thrust lever is out of consideration. Other behavioral parameters are also excluded for the low using frequency in takeoff, such as pedal angle and control wheel angle. Finally, the control column position (*CCP*) is chosen to mine from QAR data to mine ***O***. During takeoff, the ***O*** is affected by many factors such as external atmospheric environments, aircraft type, pilot basic capabilities and skills, etc. Regardless of how these factors change, their effects ultimately are reflected in the change of aircraft kinematic parameters. Therefore, according to Fig. 2 and formula (1), the flight parameters of QAR in takeoff RO risk analysis are selected from three aspects: pilot behavior (***B***), aircraft performance (***A***), and external environment (***E***). Finally, 18 flight parameter variables are chosen from QAR and calculated as shown in Table 1.

2.2. Pilot behavioral characteristics mining

In practice, pilot operates the control column at different times according to the feedback from the instruments, so the pilot behavior is time-sensitive and the operation input speed may vary from pilot to pilot. Therefore, the time series of *CCP* (*CCP_TS*) is further used to discover ***O*** and the *k*-SC time series clustering algorithm is introduced. By analyzing the shape of the cluster centers, time series clustering can reveal patterns of change in the time-series data at different moments in time. *k*-SC is a better time series clustering algorithm because its shape similarity measurement is more efficient and robust compared with other algorithms based on Euclidean Distance and Dynamic Time Warping(Yang and Leskovec, 2011).

Firstly, the *CCP_TS* when pilot manipulate the control column at the Rotation point is obtained and normalized, and the length of it is 10 s to guarantee the takeoff being finished and the requirement of *k*-SC for the same length to cluster. The optimal clustering number *k* is determined by loop based on the Elbow rule, which means the best *k* is chosen if the corresponding value of the loss function gets biggest change (Thorndike, 1953). Finally, the *S* of clustering results are analyzed by difference analysis to verify whether ***O*** has impacts on *S*. The whole process to get ***O*** is shown in Fig. 3.

2.3. The expression of *F(X)* based on similarity theory

With the consideration of ***O***, the RO risk assessment depends on an accurate description of the ***F(X)*** to get *S*. However, as a classical method, formula (1) does not consider the influence of ***O*** on ***A***, such as $P, V_R, V_{LOF}, V_2, t, C_L, C_D$, which prevents formula (1) from giving a more accurate *S*. Therefore, in order to make ***F(X)*** comprehensively reflect the influence of ***O***, ***A***, ***E***, and can be well generalized to unknow takeoff, the similarity theory based on actual flight data is introduced, which can reflect the features of RO, and be widely applied for airlines under different operation conditions. As an important scientific research method, similarity theory has been widely used in engineering field, which gives a unified expression of the system that meet same physical laws in nature. Therefore, similarity theory can make people understand the essential features between similar systems and guide people to carry out

Table 2
Parameters' dimension expressions based on 'LMT' dimension system.

Parameter	m	g	V_2	S	P	V_W	ρ	S_W
Unit	kg	$m\cdot s^{-2}$	$m\cdot s^{-1}$	m	$kg\cdot m\cdot s^{-2}$	$m\cdot s^{-1}$	$kg\cdot m^{-3}$	m^2
M	1	1	0	0	1	0	1	0
L	0	0	1	1	1	1	−3	2
T	0	−2	−1	0	−2	−1	0	0

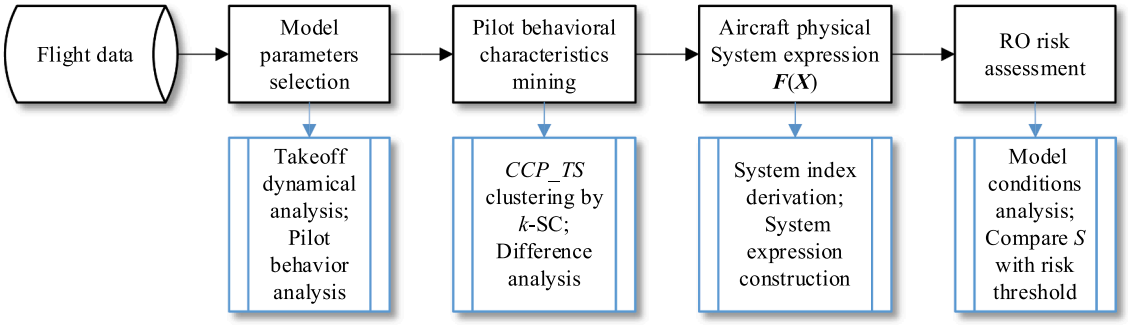

Fig. 4. Flowchart of the method.

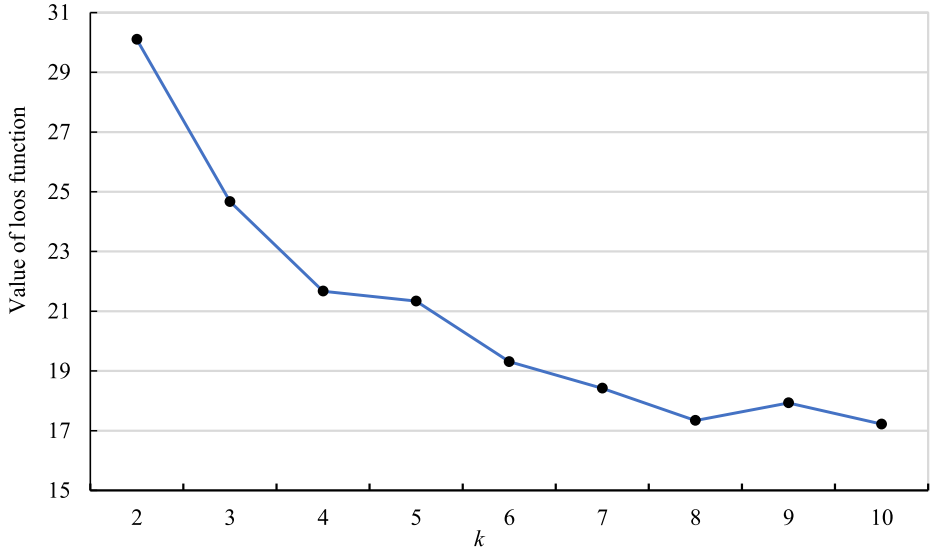

Fig. 5. The relationship between k and the value of loss function.

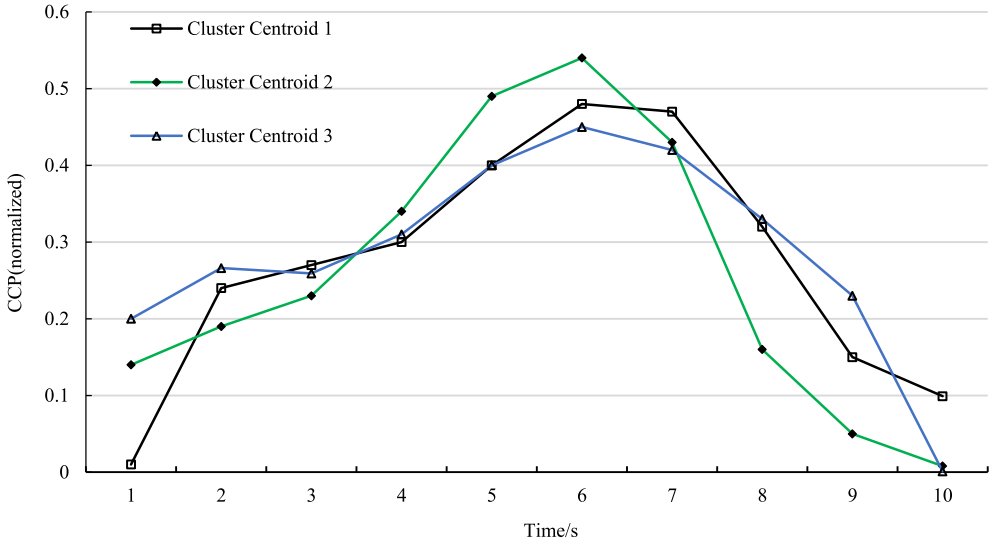

Fig. 6. Cluster centroid of *CCP_TS*.

experiments scientifically and effectively (Anderson, 2004; Pucciarelli et al., 2020; Xiao et al., 2019). Similarity theory consists mainly of the dimensional analysis and the necessary conditions which make system processes to be similar (Sedov and Volkovets, 2018). Dimensional analysis involves the construction of dimensionless index $\boldsymbol{X}$ using system parameters and the construction of $\boldsymbol{F}(\boldsymbol{X})$ based on the Buckingham Π Theorem. Similarity conditions include geometric conditions (G), media conditions (M), initial conditions (I) and boundary conditions (B). When the similarity conditions are equal, the systems are regarded as similar systems so can be analyzed by same $\boldsymbol{F}(\boldsymbol{X})$.

Table 3
One-Sample Kolmogorov-Smirnov Test.

parameter		S
N		689
Normal Parameters	Mean	1162.261
	Std. Deviation	96.832
Most Extreme Differences	Absolute	0.023
	Positive	0.019
	Negative	−0.023
Test Statistic		0.023
Asymp. Sig. (2-tailed)		0.200

Table 4
Student-Newman-Keuls Test.

Cluster centroids	N	Subset for alpha = 0.05		
		1	2	3
1	261	1133.927		
2	238		1167.931	
3	190			1194.078
Sig.		1.000	1.000	1.000

Table 5
Descriptive of $\boldsymbol{F(X)}$.

$\boldsymbol{O}$	N	Mean	Std. Deviation	Std. Error
O_1	261	1133.927	97.332	6.024
O_2	238	1167.931	87.762	5.688
O_3	190	1194.078	96.304	6.986
Total	689	1162.261	96.832	3.689

Hence, in this study, the $\boldsymbol{F(X)}$ is quantified based on dimensional analysis of flight data to build a dimensionless $\boldsymbol{F(X)}$. Then, based on the similarity conditions, all takeoffs are regarded as similar systems, including those already recorded by flight data and those planned in future. In this regard, $\boldsymbol{O}$ is innovatively considered as one of the similarity conditions. Finally, airlines can evaluate the risk of RO by calculating S in $\boldsymbol{F(X)}$, which well considers the effects of the impacts of $\boldsymbol{O}$ as well as fit the requirements of accuracy and generalization. The specific steps are detailed below.

1) Derivation of $\boldsymbol{X}$ based on dimensional analysis. The dimensional analysis $g(t)$ uses fundamental dimension of the takeoff system to represent the other variables and gives dimensionless indicators $\boldsymbol{X}$. According the formula (1) and Table 1, $\boldsymbol{X}$ is shown in formula (2):

$$\boldsymbol{X} = g(\boldsymbol{O},\boldsymbol{A},\boldsymbol{E}) = g(m,g,V_2,P,S_W,V_W,\rho,\boldsymbol{O},\mu,\varphi) \tag{2}$$

In formula (2), length(L), mass(M), and time(T) are taken as basic dimensions, and other parameters' dimensions expressed by the 'LMT' dimension system are shown in Table 2.

Select dimension independent m, g, V_2 as the basic variables. Five x_i based on dimensional analysis are shown in equations (3) ~ (7):

$$x_1 = Sm^{a_1}g^{b_1}V_2^{c_1} \tag{3}$$

$$x_2 = Pm^{a_3}g^{b_3}V_2^{c_3} \tag{4}$$

$$x_3 = V_W m^{a_2}g^{b_2}V_2^{c_2} \tag{5}$$

$$x_4 = \rho m^{a_4}g^{b_4}V_2^{c_4} \tag{6}$$

$$x_5 = S_W m^{a_5}g^{b_5}V_2^{c_5} \tag{7}$$

Take formula (3) as an example, from the Table 2 we can get formula (8):

$$\mathrm{M}^0\cdot\mathrm{L}^0\cdot\mathrm{T}^0 = \mathrm{L}\cdot(\mathrm{M})^{a_1}\left(\mathrm{L}\cdot\mathrm{T}^{-2}\right)^{b_1}\left(\mathrm{L}\cdot\mathrm{T}^{-1}\right)^{c_1} \tag{8}$$

According to the dimensional homogeneous theorem, we have formula (9):

$$\begin{cases} a_1 = 0 \\ 1 + b_1 + c_1 = 0 \\ -2b_1 - c_1 = 0 \end{cases} \tag{9}$$

Solved formula (9) we get$a_1 = 0, b_1 = 1, c_1 = -2$. Similarly, we can solve other formulas from (4) ~ (7). Five similar criterions are shown in formula (10):

$$x_1 = \frac{Sg}{V_2^2},\ x_2 = \frac{P}{mg},\ x_3 = \frac{V_W}{V_2},\ x_4 = \frac{\rho V_2^6}{mg^3},\ x_5 = \frac{S_W g^2}{V_2^4} \tag{10}$$

Since the power product of multiple similarity criteria is still the similarity criterion, the Π_4 and Π_5 are transformed. According to the B in

Table 6
ANOVA.

Model		Sum of Squares	df	Mean Square	F	Sig.
O_1	Regression	2.228	2	1.114	212.293	3.19×10^{-55}
	Residual	1.354	258	0.005	\	\
	Total	3.582	260	\	\	\
O_2	Regression	1.254	2	0.627	188.890	1.23×10^{-49}
	Residual	0.780	235	0.003	\	\
	Total	2.033	237	\	\	\
O_3	Regression	1.294	2	0.647	156.213	1.28×10^{-40}
	Residual	0.774	187	0.004	\	\
	Total	2.068	189	\	\	\

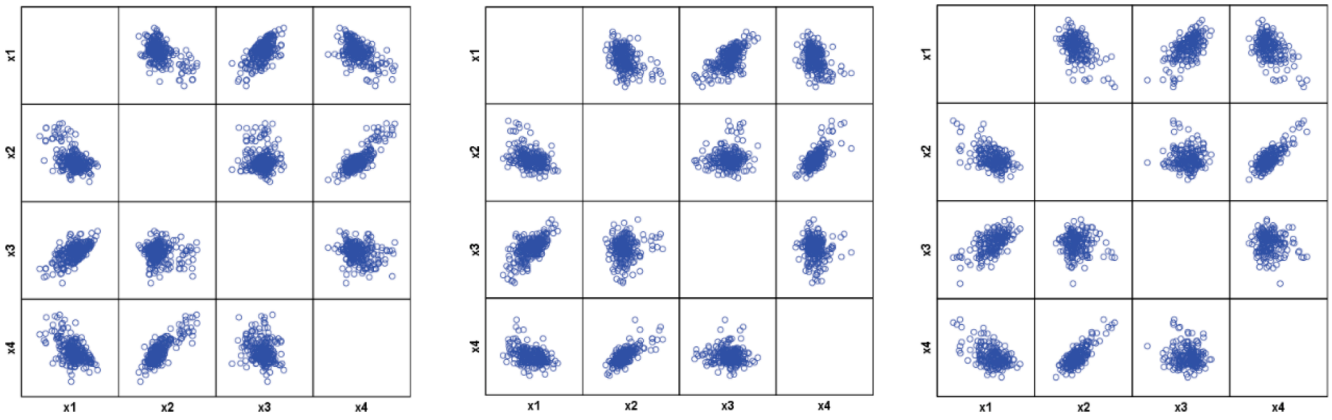

Fig. 7. Scatterplot matrices.

Table 7
Coefficients.

Model		Unstandardized Coefficients		Standardized Coefficients	t	Sig.	Collinearity Statistics	
		B	Std. Error	Beta			Tolerance	VIF
O_1	(Constant)	2.269	0.065	\	35.166	2.08×10^{-100}		\
	x_2	−4.480	0.356	−0.482	−12.580	1.26×10^{-28}	0.997	1.004
	x_3	2.796	0.180	0.596	15.548	6.51×10^{-39}	0.997	1.004
O_2	(Constant)	2.297	0.071	\	32.383	1.31×10^{-88}	\	\
	x_2	−4.504	0.396	−0.461	−11.366	3.82×10^{-24}	0.992	1.008
	x_3	2.885	0.172	0.679	16.728	6.73×10^{-42}	0.992	1.008
O_3	(Constant)	2.425	0.084		28.959	4.98×10^{-71}	\	\
	x_2	−5.258	0.469	−0.502	−11.211	1.21×10^{-22}	0.999	1.001
	x_3	2.802	0.211	0.594	13.276	9.05×10^{-29}	0.999	1.001

Table 8
Aircraft physcial system expression $\boldsymbol{F(X)}$.

$\boldsymbol{O}$	f
O_1	$x_1 = 2.269 - 4.48x_2 + 2.796x_3$
O_2	$x_1 = 2.297 - 4.504x_2 + 2.885x_3$
O_3	$x_1 = 2.425 - 5.258x_2 + 2.802x_3$

Table 9
Model Summary.

Model	R	R Square	Adjusted R Square	Std. Error of the Estimate	Durbin-Watson Statistic
O_1	0.789	0.622	0.619	0.072	1.598
O_2	0.785	0.617	0.613	0.057	1.762
O_3	0.791	0.626	0.622	0.064	1.493

similarity conditions, $\boldsymbol{O}$ is also regarded as x_k like μ andφ, finally we obtain 7 system indexes, as shown in formula (11):

$$x_1 = \frac{Sg}{V_2^2},\ x_2 = \frac{P}{mg},\ x_3 = \frac{V_W}{V_2},\ x_4 = \frac{\rho S_W V_2^2}{mg},\ x_5 = \boldsymbol{O},\ x_6 = \mu,\ x_7 = \varphi \tag{11}$$

2) The construction of $\boldsymbol{F(X)}$. Based on the Buckingham $\prod$ theorem in similarity theory, $\boldsymbol{F(X)}$ is shown in formula (12). Buckingham $\prod$ theorem is expressed as follows: the physical quantities can be expressed as a functional relationship between x_i, so we can get:

$$\boldsymbol{F}(\boldsymbol{X}) = \boldsymbol{F}(x_1, x_2, x_3, x_4, x_5, x_6, x_7) = 0 \tag{12}$$

Regard x_1 as the output of the system, we have:

$$x_1 = \boldsymbol{F}(x_2, x_3, x_4, x_5, x_6, x_7) \tag{13}$$

Formula (13) synthesizes the methodological innovations proposed in this paper, namely the construction of $\boldsymbol{F(X)}$ containing $\boldsymbol{O}$ in a dimensionless formula that express the aircraft takeoff system. In the next section, formula (13) will be further applied to assess the risk of RO.

2.4. The risk evaluation model of RO

As discussed in the introduction section, S is an important parameter in assessing RO. So, based on formula (10) and (13), we have:

$$S = \frac{V_2^2}{g}\boldsymbol{F}(x_2, x_3, x_4, x_5, x_6, x_7) \tag{14}$$

S can be calculated based on formula (14) and thus assess the risk of RO by comparing it to the set risk threshold. However, formula (14) only reflects the essential principle of motion embedded between takeoff systems. For the $\boldsymbol{F(X)}$ fitted based on known takeoff data (Know-Takeoff), the similarity between Know-Takeoff and Unknow-Takeoff must be satisfied to more accuracy describe the Unknow-Takeoff. Similarity theory states that systems are similar if the similarity conditions are numerically equal. So, based on the similarity conditions, we divide the original takeoff dataset $\boldsymbol{D}$ into the reference dataset D_i, then Know-Takeoff and Unknow-Takeoff are similar withinD_i. Therefore, the $\boldsymbol{F(X)}$ fitted based on the reference dataset can be generalized to the Unknow-Takeoff.

Concretely, according to the B in similarity conditions, we set $\boldsymbol{O}, \mu, \varphi$ in formula (14) as in category quantities based on original dataset. Meanwhile, other similarity conditions are set as follows:

- M: operating in the atmosphere, the system has been satisfied.
- G: same specific aircraft type and Flap.
- I: this condition has been met by the system as the aircraft starts takeoff from standstill.

Then, the original QAR dataset $\boldsymbol{D}$ can be divided into a set of reference dataset D_i, $i = 1, 2, \ldots n$, and the physical process of takeoff is assumed to be similar in D_i. In D_i we have:

$$x_1 = f_i(x_2, x_3, x_4) \tag{15}$$

$$S = \frac{V_2^2}{g} f_i(x_2, x_3, x_4) \tag{16}$$

Therefore, based on D_i and the formula (15), a series of equations of $\boldsymbol{F} = \{f_1, f_2, \ldots, f_n\}$ can be fitted in D_i. By using the fitted formulas and the similar relationship between Know-Takeoff and Unknow-Takeoff, S under specific similarity conditions based on formula (16) can be evaluated. Thus far, based on similarity theory, we have obtained the necessary conditions and a calculation model for assessing future RO risk based on the available QAR data. The flowchart process of the entire method is shown in Fig. 4.

3. Case study

Overall, the real flight data for our study were obtained from an airline in Tianjin, China, whose main operating aircraft is Boeing 737–800 and is based at Tianjin Binhai International Airport. We obtained approximately 1000 cases of raw QAR samples, each recording real flight parameters includes $\boldsymbol{B}$, $\boldsymbol{A}$ and $\boldsymbol{E}$ of a complete flight process. In order to verify the feasibility of the method proposed in this study, the raw data are screened based on the necessary conditions presented in section 2.4. As the study objectives already satisfied the medium and initial conditions(M&I), we further filtered the raw data based on geometric and boundary conditions(G&B) as follows:

1) Same aircraft type and takeoff configuration. In sample data, the aircraft type is B737-800 and the flaps configuration is 5;

2) The slope of runway is same and the runway is dry. Screening of airports with same slope based on the Departure Airport parameter in QAR and filtering the cases by Departure Date parameter in QAR for precipitation and foggy weather to maximize dry runway conditions and departure visibility requirements. Takeoff samples on sunny days from June to August is selected to adequately meet dry runway conditions;

3) The tailwind component at the airport is less than 5 m/s. Usually too much wind speed may have a negative impact on the takeoff. For

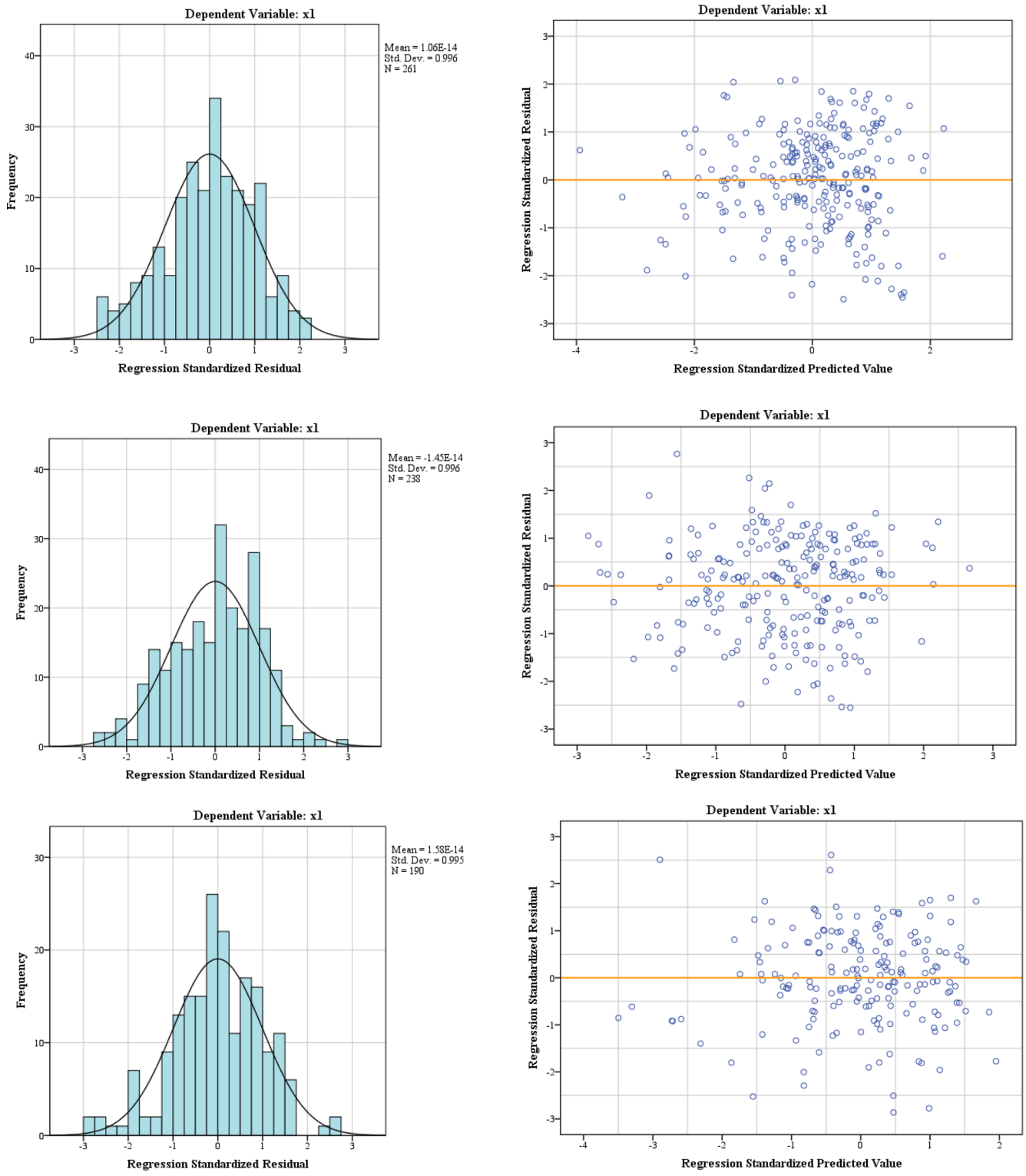

Fig. 8. Residual analysis diagram.

instance, a downwind takeoff increases the takeoff distance and a sidewind takeoff increases the pilot's operational load. Conversely, a headwind helps the aircraft to get off the ground quickly. The case study considers normal conditions to discover the general $\boldsymbol{O}$, so we left out excessive wind speeds for the time being. Based on the performance reference data for the B737-800 (BRADY, 2021), no effects on aircraft takeoff safety when the tailwind speed is below 10 kts (5.14 m/s). Therefore, we artificially set the tailwind component threshold as 5 m/s in the case study section, with the tailwind being calculated based on Wind Speed and Wind Direction in QAR.

Finally, 689 flight samples were selected, which supports two parts of results presented in this section. The section 3.1 shows the results of k-SC clustering analysis and the final derived $\boldsymbol{O}$. In section 3.2, the $\boldsymbol{F}(\boldsymbol{X})$ is delivered based on multipule regression, and the RO risk assessment results are given by calculating S in section 3.3.

Table 10
Assessment model of S.

O	f
O_1	$S = \frac{V_2^2}{g}(2.269 - 4.48x_2 + 2.796x_3)$
O_2	$S = \frac{V_2^2}{g}(2.297 - 4.504x_2 + 2.885x_3)$
O_3	$S = \frac{V_2^2}{g}(2.425 - 5.258x_2 + 2.802x_3)$

Table 11
Model performance comparison in text airport.

Model	Mean absolute error/m	Root Mean square error/m	Mean relative error /%	Maximum absolute error/m	Maximum relative error/%
O_1	17.58	22.95	1.47	49.22	4.59
O_2	20.11	23.53	1.90	34.55	4.06
O_3	32.80	36.60	3.39	51.17	5.39

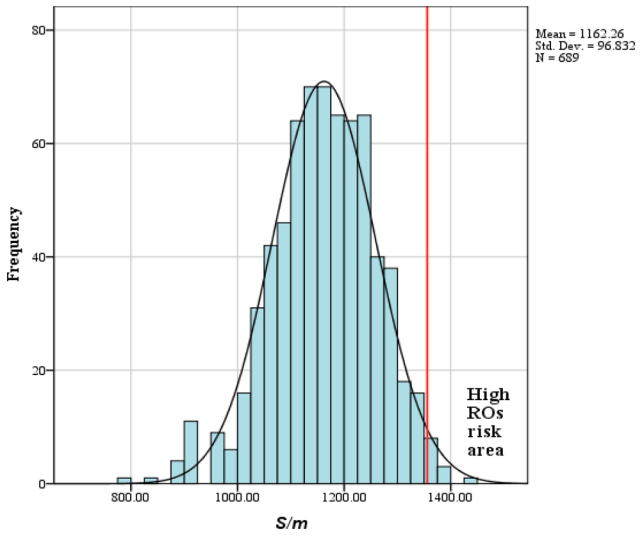

Fig. 9. Threshold setting of RO.

3.1. Pilot behavioral characteristics

According to Fig. 3, 689 *CCP_TS* samples were normalised and the $k_{\min}$ in k-SC was settled as 2. The k-SC algorithm was executed until $k = 10$. Fig. 5 shows the relationship between the value of loss function and k, and the biggest change of the curve appears when k equals 3. The result of k-SC based on $k = 3$ is shown in Fig. 6.

As we can see from Fig. 6, all the three cluster centroids appear similar trend after V_R. However, there are some main differences in the shape of the centroids, which are reflected by the initial column position and the change of rate. Cluster centroid 1 pulls the column lately, for the *CCP* in *VR* are smaller than others, and the *CCP* in last second is also the biggest one. Meanwhile, its pulling speed is fastest at *VR*. Cluster centroid 2 reflects a more rapid column change rate in average. Compared with others, cluster 3 represents a gender and advanced column operation because of the earliest and moderate column operating speed.

The difference analysis was made to further judge whether the three cluster centroids have differences in S. The result of the K-S test of S in selected samples is shown in the Table 3, which means S conforms to a normal distribution with a mean of 1162.261 m and a standard deviation of 96.832 m. The result of Student-Newman-Keuls Test is shown in Table 4.

The Table 4 shows that S of three clusters have significant difference so that three kinds of $\boldsymbol{O}$ are got, and the descriptive in Table 5 indicates that O_3 has the largest S compared with others and O_1 does vice versa.

3.2. The mathematical description of the aircraft takeoff system

In sample data, the slope of runway is same and the runway is dry, so the reference data was divided into three groups by attained $\boldsymbol{O}$. The relationships bewteen other 4 similarity crierions in formula (15) are shown in Fig. 7, which display linear relationship to some extent so the multiple liner regression was used to fit formula (15).

The multiple linear relationship regression results of different $\boldsymbol{O}$ are shown in Tables 6-9.

The ANOVA shows that it is reliable to use the multiple liner regression to fit f in formula (15), and the coefficients in Table 8 are all significant after excluded x_4 in formula (15) by stepforward regression method. The final equations based on formula (15) are displayed in Table 8 and the adjusted R Square in Table 9 means that the equations have an acceptable performance. Besides, the Durbin-Watson Statistic values in Table 9 and the residual analyze in Fig. 8 further illustrate that the equations fit the necessary conditions of using multiple liner regression model, which are normality, independence, homogeneity of variance. No collinearity be found according the VIF in Table 7.

3.3. The risk assessment model of RO

Based on the Table 8 and formular (16), the assessment model of S is shown in Table 10.

The evaluation results of the prediction models in test airport are shown in Table 11, which means the effectiveness of the model is acceptable to some degree. This further demonstrates that S can be predicted more accurately based on our model and thus the RO risk of the aircraft can be effectively assessed.

Based on the distribution of S in current fleet, the threshold for RO is set at 1355.92 based on 2 times the standard deviation, as shown in Fig. 9. when S in Table 10 is higher than the threshold, the risk of RO is considered high.

4. Discussion

Pilot behavior is always an important factor in flight safety. The aircraft takeoff safety depends on the performance of pilot behavior so $\boldsymbol{O}$ should be considered when analyzing RO risk. At the same time, RO risk assessment methods should be highly accurate and well generalized. Based on real flight data, we have achieved the above objectives and the realization process will be fully discussed. In this part, the discussion about $\boldsymbol{O}$ is given in section 4.1. The aircraft takeoff system expression $\boldsymbol{F}(\boldsymbol{X})$ embedded $\boldsymbol{O}$ will be discussed in section 4.2, and the final risk assessment model of RO is discussed in section 4.3.

4.1. Pilot behavioral characteristics based on flight data

The definition, the analytical methods, and limitations of $\boldsymbol{O}$ will be fully discussed. The defined $\boldsymbol{O}$ describes the impacts of pilot behavior on aircraft, which comprehensively reflects the management level of the airline, including flight training, regulations, management culture, etc. All QAR operating parameters can reflect $\boldsymbol{O}$, such as control column position, throttle resolver angle, pedal angle, and steering wheel angle, etc. Therefore, more operational data could be used to complete the mining of $\boldsymbol{O}$ in future studies. In current study, *CCP_TS* is selected to discover $\boldsymbol{O}$, which can essentially reflect the time and speed of pilot control column manipulation during takeoff. In concrete method, the $k_{\max}$ in Fig. 3 is limited to 10 due to data volume and computing power limitations. In fact, the amount of QAR data from Chinese airlines can reach terabyte level per day, which means we can mine $\boldsymbol{O}$ with the

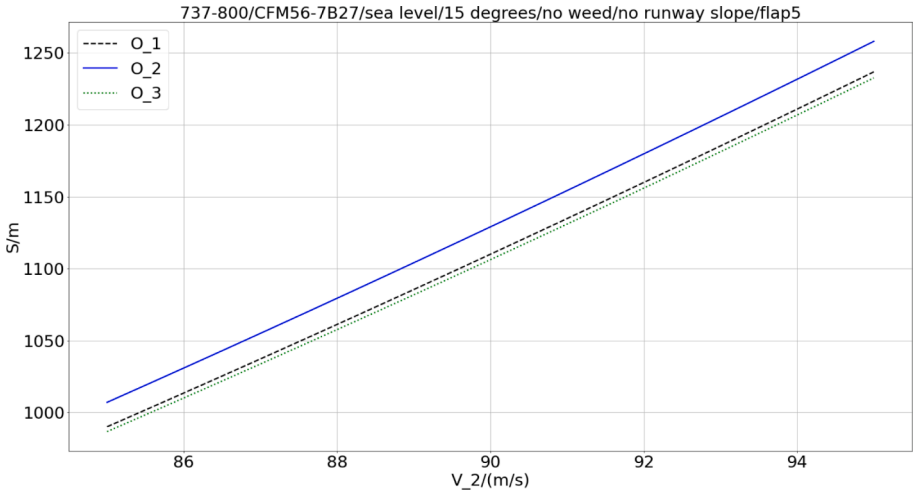

(a) m=60000kg; $V_W = 0\text{m}\cdot\text{s}^{-1}$; $P = 27300\text{N}$; ρ=1.225 $\text{kg}\cdot\text{m}^{-3}$

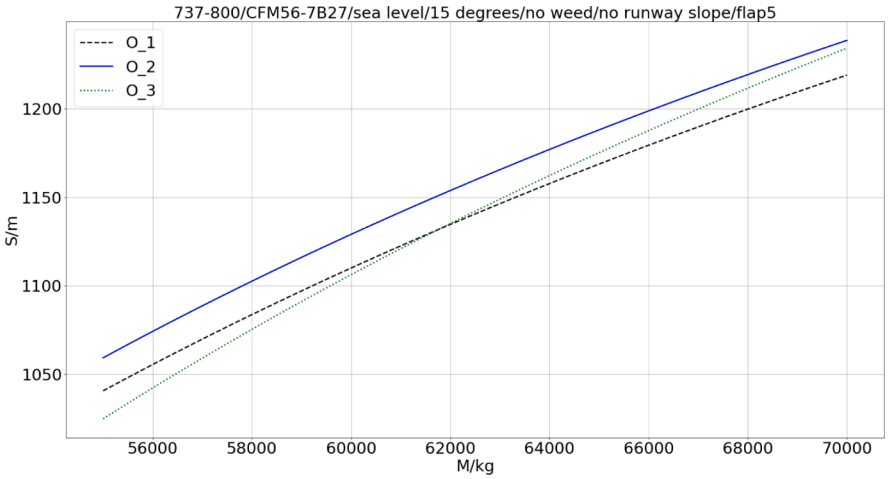

(b) V_2=90$\text{m}\cdot\text{s}^{-1}$; $V_W = 0\text{m}\cdot\text{s}^{-1}$; $P = 27300\text{N}$; ρ=1.225 $\text{kg}\cdot\text{m}^{-3}$

Fig. 10. Performance comparison diagram of ***O***.

support of high-performance computers in the future and could get more interesting results. From Fig. 6 and Table 5, we can conclude that timely and faster pulling up after the Rotation point helps to reduce*S*, which is consistent with the law of motion of aircraft. A 'just-in-time pull' indicates that the shorter pilot reaction time to make a pull when the instruments indicate pilot to rotate, the shorter *S* due to inertia within the corresponding time. A 'fast pull' adds the rate of the increase in lift, resulting in an increase in altitude per unit time, and therefore the shorter the horizontal distance travelled by the aircraft. The conclusion is consistent with the results of the literature (Wang et al., 2018), which indicates that pilots' faster and steady backward pulling on columns is helpful for a better flare and landing. In our cases, pilot reaction time and operational stability have a significant impact on aircraft operation, which are underlying influenced by various factors such as psychological factors, physiological factors, and airline management, making the mechanistic analysis of ***O*** become more complex. Therefore, future research needs to focus on the cognitive processes of analysts to discover the causes of ***O*** and to control high risk ***O*** by the methods like psychological interventions and improved flight training. In practice, ***O*** can be annotated with pilots to analyze accident risks before his or her next flight, which is of great significance for the further improvement of the safety level of civil aviation.

4.2. System expression based on human–machine-environment factors

S is an important parameter in assessing the aircraft performance and the length of runway, so *S* is key to the runway safety. As the equipment reliability continues to increase, the pilot behavior is increasingly becoming a key factor influencing *S* while the existing studies often fail to incorporate pilot behavior into system safety analysis. Based on the obtained ***O*** and combined with the similarity theory, the study summarizes the human–machine-environment factors affecting *S* into one mathematical model and apply it to access RO risk. In contrast to data-based fitting methods, similarity theory has following advantages. First, the system indexes constructed by the similarity theory are dimensionless, which reducing the number and correlation of system indexes and the complexity of fitting ***F***(***X***). Second, the similarity theory can scientifically guide the division of experimental data so that the f_i could have better accuracy and generalization. The proposed model can not only reduce the correlation between system indexes and then built dimensionless ***F***(***X***), but also give detailed application conditions of ***F***(***X***). The model is constructed based on the real flight data, which objectively restored the real flight routine of pilots, so has practical significance. The result of multiple regression indicated that the ***F***(***X***) is consistent with the physical rules of takeoff, for all the fitting equations delet the

regression coefficient of indimentional critierion's include air density, which is consistent to the use of true airspeed in our method. The coefficients in Table 8 also show that, at the sameV_2, an increase in thrust-to-weight ratio has a negative effect on the increase in S and an increase in runway headwind speed has a positive effect on the increase in takeoff distance. As we can see in Table 10, our model finally has good prediction preference in different $\boldsymbol{O}$ and the Fig. 10 shows intuitively that $\boldsymbol{O}$ does have an effect on S in different control conditions. As discussed previously, it is the different pilot reaction time and operation input speed that cause differences in S under controlled conditions.

The case analysis didn't further fit more f_i under different runway friction coefficient and runway slope. At the same time, due to the data volume, the case analysis failed to consider more similarity conditions, such as different configuration settings, aircraft types, weather conditions, etc. In future, the model under more similarity conditions will be constructed based on the massive flight data of airlines, to further improve the application scope. Besides, as another vital stage, landing could also be considered and our method could be a reference to solve the problems like mining the landing behavioral characteristics of landing RO assessment and other unsafety events such as hard landing and tail strike.

4.3. RO risk assessment based on pilot behavior

Human factors are always an important aspect of flight accident risk analysis(Burns and Bonaceto, 2020; Erjavac et al., 2018). This study emphasizes the influence of human behavioral characteristics on the system safety and incorporates them into system expression. The objective of system operational risk from the perspective of human–machine-environment is given. In the field of flight safety, the RO is always a high-risk incident and evaluating S is always an important technical tool for assessing the risk of RO. However, most studies tend to focus more on equipment and environmentally factors to improve system safety of runway operation while ignoring the impact of pilot behavior to some degree. At the same time, even though pilot behavior has been summarized in accident statistics as a factor influencing RO, there has been no quantitative analysis based on real flight data. In this study, the $\boldsymbol{O}$ is explored based on objective data, which improving the effectiveness of takeoff RO risk assessment based on the human behavior. For risk assessment issues, a reasonable selection of risk thresholds is important. There are limitations to this study in selecting a fixed RO risk threshold based on the distribution of S, because the definition of safety risk thresholds also should consider the effects of pilot behavior. The pilot risky behavior causes constant fluctuations in safety thresholds and safety managers must continuously monitor the behavioral characteristics of high-risk pilots and adjust existing thresholds for the risk of unsafe events to further ensure the flight safety.

5. Conclusions

Compared to the qualitative results based on statistics in the current study, based on real flight data, this study found that the $\boldsymbol{O}$ do have an impact on the risk of takeoff runway overruns in aviation safety and obtained a quantitative risk calculation method of RO. 3 types of $\boldsymbol{O}$ were discovered in selected fleet, which show that pilot reaction time after V_R and operation input speed are the main behavioral characteristics during takeoff. Longer pilot reaction times are always accompanied by slower operation input speeds, which put the aircraft at increased risk of RO. At the same time, the proposed method can make full use of the huge amount of flight data from airlines with different conditions to construct a more accurate risk assessment model for RO. The method is of reference value to other aviation safety events of risk analysis considering human behavior.

CRediT authorship contribution statement

Chongfeng Li: Writing – original draft, Visualization, Validation, Software, Investigation, Funding acquisition, Formal analysis, Data curation. **Ruishan Sun:** Methodology, Conceptualization. **Xing Pan:** Writing – review & editing, Supervision.

Declaration of Competing Interest

The authors declare that they have no known competing financial interests or personal relationships that could have appeared to influence the work reported in this paper.

Acknowledgements

Our gratitude goes out to the local airlines for providing us with data, even though it is confidential for them.

References

Anderson, D., 2004. Manual of Scaling Methods, NASA/CR-2004-212875.
Ayres, M., 2011. Improved Models for Risk Assessment of Runway Safety Areas. Transportation Research Board.
Bateman, D., 2008. A Review of some Technological Aids to Support the Flight Safety Foundation Runway Safety Initiative (RSI), FSF 61st Annual International Air Safety Seminar (IASS). Honolulu, Hawaii, pp. 1–24.
BRADY, C., 2021. The Boeing 737 technical guide. http://www.b737.org.uk/limitations.htm#Wind_Limit.
Burns, K., Bonaceto, C., 2020. An empirically benchmarked human reliability analysis of general aviation. Reliab. Eng. Syst. Saf. 194, 106227.
Caac, 2021. Aviation Safety Report of CAAC. Civil Aviation Administration of China, Beijing.
Cai, L.C., Wang, W.F., Zhu, Z.Q., Chong, X.L., 2013. Calculation method of running distance for aircraft takeoff on plateau airport. J. Traffic Transport. Eng. 13, 66–72.
Calle-Alonso, F., Pérez, C.J., Ayra, E.S., 2019. A Bayesian-network-based approach to risk analysis in runway excursions. J. Navigat. 72, 1121–1139.
Chang, Y.-H., Yang, H.-H., Hsiao, Y.-J., 2016. Human risk factors associated with pilots in runway excursions. Acc. Anal. Prevent. 94, 227–237.
Chen, C.-F., Chen, S.-C., 2014. Measuring the effects of Safety Management System practices, morality leadership and self-efficacy on pilots' safety behaviors: Safety motivation as a mediator. Saf. Sci. 62, 376–385.
Chen, H., Xiang, X., 2013. Discussion of civil aircrafts operating landing distance calculation method. Comput. Simulat. 30, 66–69.
De Sant, D.A.L.M., De Hilal, A.V.G., 2021. The impact of human factors on pilots' safety behavior in offshore aviation companies: a brazilian case. Saf. Sci. 140, 105272.
Dekker, S.W., 2001. The re-invention of human error. Human Factors Aerospace Saf. 1, 247–265.
Di Mascio, P., Cosciotti, M., Fusco, R., Moretti, L., 2020. Runway veer-off risk analysis: An international airport case study. Sustainability 12, 9360.
Erjavac, A.J., Iammartino, R., Fossaceca, J.M., 2018. Evaluation of preconditions affecting symptomatic human error in general aviation and air carrier aviation accidents. Reliab. Eng. Syst. Saf. 178, 156–163.
Dolores, Gracja, P., 2018. Human factor in flight safety. Hadmérnök 13, 381–396.
European Aviation Safety Agency, 2016a. Annual Safety Review 2016.
European Aviation Safety Agency, 2016b. European Plan for Aviation Safety 2016–2020.
Galagedera, S., Pasindu, H., Adikariwattage, V., 2019. Analysis of aircraft veer off probability at runway high speed exits, 2019 Moratuwa Engineering Research Conference (MERCon). IEEE 527–532.
Galagedera, S., Pasindu, H., Adikariwattage, V., 2020. Evaluation of operational risk factors at runway high speed exits. Transp. Res. Procedia 48, 32–46.
Gandhewar, P., Sonkusare, H.G., 2014. Runway excursion: a problem. IOSR J. Mech. Civ. Eng 11, 75–78.
Hobbs, A., 2004. Human factors: the last frontier of aviation safety? Int. J. Aviation Psychol. 14, 331–345.
Hong, C., Mingliang, Q., Xueyan, S., 2011. Flight operations risk diagnosis method on quick-access-record exceedance. J. Beijing Univ. Aeronautics Astronaut.
International Air Transport Association, 2011a. Runway excursion analysis report 2004–2009.
International Air Transport Association, 2011b. Runway excursion risk reduction toolkit.
International Civil Aviation Organization, 2013. Annex 14: Aerodrome Design and Operations.
IATA, 2021. Safety report 2020. International Air Transport Association, Montreal, Canada.
Jarvis, S., Harris, D., 2010. Development of a bespoke human factors taxonomy for gliding accident analysis and its revelations about highly inexperienced UK glider pilots. Ergonomics 53, 294–303.
Jensen, R.S., 2017. Pilot judgment and crew resource management. Routledge.
Lee, S., Kim, J.K.J.J.o.a.t.m., 2018. Factors contributing to the risk of airline pilot fatigue. Journal of air transport management 67, 197-207.

Lone, M., Cooke, A., 2014. Review of pilot models used in aircraft flight dynamics. Aerospace Sci. Technol. 34, 55–74.
Madeira, T., Melício, R., Valério, D., Santos, L., 2021. Machine learning and natural language processing for prediction of human factors in aviation incident reports. Aerospace 8, 47.
Moretti, L., Cantisani, G., Caro, S., 2017a. Airport veer-off risk assessment: An Italian case study. ARPN J. Eng. Appl. Sci 12, 900–912.
Moretti, L., Cantisani, G., Di Mascio, P., Nichele, S., Caro, S., 2017b. A runway veer-off risk assessment based on frequency model: Part I. Probability analysis, Transport infrastructure and systems. CRC Press, pp. 515–522.
Moretti, L., Cantisani, G., Di Mascio, P., Nichele, S., Caro, S., 2017c. A runway veer-off risk assessment based on frequency model: Part II. risk analysis, Transport Infrastructure and Systems. CRC Press, pp. 523–528.
Moretti, L., Di Mascio, P., Nichele, S., Cokorilo, O., 2018. Runway veer-off accidents: Quantitative risk assessment and risk reduction measures. Saf. Sci. 104, 157–163.
NLR, 2015. Identification and analysis of veer-off risk factors in accidents/incidents. Netherlands Aerospace Centre.
Natalia, D., Salvatore, L., 2020. Apriori algorithm for association rules mining in aircraft runway excursions. Civ. Eng. Archit 8, 206–217.
Pucciarelli, A., Ambrosini, W.J.I.j.o.h., transfer, m., 2020. A successful general fluid-to-fluid similarity theory for heat transfer at supercritical pressure. International journal of heat 159, 120152.
Qian, S., Zhou, S., Chang, W., Wei, F., 2017. An improved aircraft landing distance prediction model based on particle swarm optimization—Extreme learning machine method, 2017 IEEE International Conference on Industrial Engineering and Engineering Management (IEEM). IEEE, pp. 2326-2330.
Reason, J., 1990. Human error. Cambridge University Press.
Ruiying, W., Bo, W., Shuanglei, C., Hongyong, W., 2017. Prediction of landing distance for civil aircraft. China Saf. Sci. J. 27, 77.
Sagberg, F., Selpi, Bianchi Piccinini, G.F., Engström, J.J.H.f., 2015. A review of research on driving styles and road safety. Human factors 57, 1248-1275.
Santos, L., Melicio, R., 2019. Stress, pressure and fatigue on aircraft maintenance personal.
Sedov, L.I., Volkovets, A., 2018. Similarity and dimensional methods in mechanics. CRC Press.
Shappell, S., Detwiler, C., Holcomb, K., Hackworth, C., Boquet, A., Wiegmann, D.A., 2017. Human error and commercial aviation accidents: an analysis using the human factors analysis and classification system. Human error in aviation. Routledge 73–88.
Skybrary, 2022. Runway Excursion. https://skybrary.aero/articles/runway-excursion.
Song, H.Y., Cai, L.C., Zheng, R.H., 2007. Numerical value integral improvement algorithm of aircraft take-off running distance. J. Traffic Transport. Eng. 7, 24–28.
Sun, R., Xiao, Y., 2012. Research on indicating structure for operation characteristic of civil aviation pilots based on QAR data. J. Saf. Sci. Technol. 8, 49–54.
Szabo, S., Vittek, P., Kraus, J., Plos, V., Lališ, A., Štumper, M., Vajdova, I., 2017. Probabilistic model for airport runway safety areas. Transport Probl. 12, 32–46.
Thorndike, R.L., 1953. Who belongs in the family. Psychometrika, Citeseer.
Thorpe, A., Estival, D., Molesworth, B., Eidels, A., 2022. Pilot errors: communication comes last. Saf. Sci. 149, 105686.
Volz, K., Yang, E., Dudley, R., Lynch, E., Dropps, M., Dorneich, M.C., 2016. An evaluation of cognitive skill degradation in information automation, proceedings of the human factors and ergonomics society annual meeting. SAGE Publications Sage CA, Los Angeles, CA, pp. 191–195.
Wang, L., Wu, C., Sun, R., 2013. Pilot operating characteristics analysis of long landing based on flight QAR data. In: International Conference on Engineering Psychology and Cognitive Ergonomics. Springer, pp. 157–166.
Wang, L., Ren, Y., Wu, C., 2018. Effects of flare operation on landing safety: A study based on ANOVA of real flight data. Saf. Sci. 102, 14–25.
Wei, Y.-Z., Chong, X.-L., Liu, W., Guo, S.-F., Guo, L.-G., 2018. Risk Assessment of Separation Between Runway and Taxiway Not Meeting Standard During Take-off, IOP Conference Series: Earth and Environmental Science. IOP Publishing, p. 032013.
Xiao, Z., Liang, Z., Li, B., Hou, B., Hu, Y., Wang, J., 2019. New flood early warning and forecasting method based on similarity theory. J. Hydrol. Eng. 24, 04019023.
Xu, S., Tan, W., Efremov, A.V., Sun, L., Qu, X., 2017. Review of control models for human pilot behavior. Ann. Rev. Control 44, 274–291.
Xu, Q., Wu, Y., Wang, M., Liu, B., Jiang, J., You, X., Ji, M., 2022. The relationship between sense of calling and safety behavior among airline pilots: the role of harmonious safety passion and safety climate. Saf. Sci. 150, 105718.
Yang, J., Leskovec, J., 2011. Patterns of temporal variation in online media, Proceedings of the fourth ACM international conference on Web search and data mining, pp. 177-186.
Yazgan, E., Kavsaoğlu, M.Ş., 2017. Evaluation of stress affecting aircraft maintenance technician" s performance. Int. J. Comput. Commun. Instrum. Eng. 4, 2349–2469.
Yousefi, Y., Karballaeezadeh, N., Moazami, D., Sanaei Zahed, A., Mohammadzadeh, S.D., Mosavi, A., 2020. Improving aviation safety through modeling accident risk assessment of runway. Int. J. Environ. Res. Public Health 17, 6085.
Zhu, T., Tong, Z., 2021. FOBA: flight operation behavior analysis based on hierarchical encoding. Int. Conf. Knowledge Sci. Eng. Manage. Springer 205–217.